

# Spectral Properties of Directed Random Networks with Modular Structure

Sarika Jalan\*

*School of Sciences, Indian Institute of Technology Indore,  
IET-DAVV Campus Khandwa Road, Indore 452017, India and  
Department of Physics and Centre for Computational Science and Engineering,  
National University of Singapore, 117456, Republic of Singapore*

Guimei Zhu<sup>†</sup> and Baowen Li<sup>‡</sup>

*NUS Graduate School for Integrative Sciences and Engineering, 117456, Republic of Singapore and  
Department of Physics and Centre for Computational Science and Engineering,  
National University of Singapore, 117546, Republic of Singapore*

We study spectra of directed networks with inhibitory and excitatory couplings. We investigate in particular eigenvector localization properties of various model networks for different value of correlation among their entries. Spectra of random networks, with completely uncorrelated entries show a circular distribution with delocalized eigenvectors, where as networks with correlated entries have localized eigenvectors. In order to understand the origin of localization we track the spectra as a function of connection probability and directionality. As connections are made directed, eigenstates start occurring in complex conjugate pairs and the eigenvalue distribution combined with the localization measure shows a rich pattern. Moreover, for a very well distinguished community structure, the whole spectrum is localized except few eigenstates at boundary of the circular distribution. As the network deviates from the community structure there is a sudden change in the localization property for a very small value of deformation from the perfect community structure. We search for this effect for the whole range of correlation strengths and for different community configurations. Furthermore, we investigate spectral properties of a metabolic network of zebrafish, and compare them with those of the model networks.

PACS numbers: 89.75.Hc, 89.90.+n

## I. INTRODUCTION

Statistical properties of large random matrices have been investigated intensively since the early 1950s and have turned out to be valuable tools for both qualitative and quantitative descriptions of spectral properties of complex systems [1]. Examples include, complicated interactions in nuclei, quantum mechanical aspects of chaos, and the stock market. Recent success has been achieved in systems having an underlying network structure [2]. In applications of random matrix theory to physical problems, it is generally assumed that the details of the physical systems are less important for many statistical properties of interest. Often it turns out that important statistical properties such as the distribution of eigenvalues or the spacings of energy levels in quantum systems are well described by the respective properties of random matrices that respect the same symmetries as the physical system [3].

Recent investigations of statistical properties of eigenvalues of networks show that bulk eigenvalue spacings follow Gaussian orthogonal ensemble (GOE) predictions of random matrix theory (RMT) [4–6], whereas the eigenvalue distribution itself depend on network properties

[5–9]. These analyses show that the spectral distributions of bulk eigenvalues of random networks follow Wigner’s semi circular distribution, for scalefree networks [10] the bulk eigenvalues follow a triangular distribution, for smallworld networks [11] they form a multi peak distribution, and for realworld networks they show one of the above mentioned distributions with a high peak at zero eigenvalues [5, 9]. Further investigations of the community structure in networks show the transition to Wigner’s semi circular distribution as the community structure is destroyed. Even a very small deformation from the community structure gets captured by the eigenvalues distribution [12].

All the above investigations have been performed for undirected networks leading to a symmetric adjacency matrix and for which eigenvalues are real. Many complex systems are described by directed networks [13], for example, the World Wide Web, neural networks, protein interaction networks and many social networks are directed or asymmetrically weighted, and hence lead to complex eigenvalues of the corresponding adjacency matrices. One of the most important features shown by realworld networks is the existence of modular or community structures [14–16]. The study of community structures helps to elucidate the organization of networks, and eventually could be related to the functionality of groups of nodes. Regardless of the type of realworld networks in terms of the degree and other structural properties [13], it is possible to distinguish communities throughout the whole networks [14]. However, the question of the defini-

---

\*Electronic address: sarikajalan9@gmail.com

<sup>†</sup>Electronic address: zhugm07@gmail.com

<sup>‡</sup>Electronic address: phylibw@nus.edu.sg

tion of the community is problematic. Usually community is assigned to the nodes that are connected densely among themselves, and are only sparsely connected with other nodes outside the community.

So far most of the theoretical investigations and applications of RMT have focused on symmetric matrices. Asymmetric matrices or non-Hermitian matrices are less well understood. A classic result for non-Hermitian matrices in random matrix theory is Girko's circle law [17] which states that, for large  $N$ , the eigenvalues of an  $N \times N$  asymmetric matrix lie uniformly within the unit circle in the complex plane, if the elements are chosen from a distribution with zero mean and variance  $1/N$ . When partial symmetry is included, the circle changes to an ellipse [18]. Recently, numerical studies on spectral properties of asymmetric matrices have been done in the context of Google networks [19, 20]. Additionally the spectral density of non-Hermitian sparse matrices has been analyzed in the Ref. [21].

In this paper we evaluate the applicability of RMT for the distribution of eigenvalues of directed networks where entries in the corresponding matrix take values motivated by inhibitory and excitatory coupling between nodes. In particular, we investigate spectral properties of directed networks having a community structure. The matrix corresponding to these networks is different from the non-Hermitian random matrices studied under a RMT framework. The main differences are that (a) the matrix is not *random*, i.e. the position of entries in the matrix depends on the underlying network structure; (b) real world networks and model networks are sparse and consequently most of the entries in the corresponding matrix are zero; and (c) most importantly, the entries in the matrix take values 0,  $-1$  and  $1$ . These entries are motivated by the excitatory and inhibitory synapse between neurons leading to positive and negative values of the connections between them.

The spectra of matrices having entries 0, 1 and  $-1$ , known as Seidel matrices, have been investigated intensively in the literature. In graph theory, the Seidel adjacency matrix of a simple graph  $G$  is a symmetric matrix having 0 at the diagonal entries,  $G_{ij} = -1$  if node  $i$  is neighbor of node  $j$ , and other entries of this matrix taking the value 1. For Seidel matrices  $G_{ij} = G_{ji}$ . The multiset of eigenvalues of this matrix is called the Seidel spectrum. The Seidel matrix was introduced by van Lint and Seidel [22] and extensively exploited by Seidel and co-workers. Seidel matrix provides insight to the properties of graphs, thus leading to several applications such as modeling social situations, spin glasses in physics, and clustering of data [23].

Note that, except for the matrix entries being binary 1,  $-1$  and 0, Seidel matrices are completely different from the matrix representation considered in the present paper. The first difference between Seidel matrices and the matrices investigated herein is that the latter are directed (asymmetric) matrices, i.e.,  $A_{ij} \neq A_{ji}$  depending upon the value of  $\tau$ , a measure of directionality or correlation.

Consequently, we get complex eigenvalues following the universal Girko's law for the case when the matrix is completely uncorrelated. The second most important difference is that we have  $A_{ij} = 0$  for the nodes that are not connected, i.e., vertices that are not neighbors, whereas Seidel matrices have the entries 1 for non neighboring nodes. This second property of our matrices again leads to a very crucial difference called 'sparseness', which affects the spectral properties to a great extent in comparison to the matrices corresponding to fully connected networks. The third important difference between the matrix we have considered in this paper and the Seidel matrices we found in the literature is the underlying structure: Seidel matrices are mostly investigated for regular graphs (such as strong regular graphs and two-graphs) [24], whereas the matrices that we are investigating in the paper are *random with some structure*, corresponding to ER graphs, BA scalefree graphs, modular graphs and modular realworld networks. There are cases in the literature where the Seidel matrix of ER graphs and realworld graphs have been investigated; in the following we provide details of these studies only, as they seem to be close to our studies at least in terms of the structure of the underlying network (Seidel matrices of random graphs have been studied mainly for the graph bisection problem.) Reference [25] shows through numerical analysis that Seidel representations produce the smallest cuts for random ER graphs than other representations such as the adjacency and Laplacian matrices.

Spectral densities of directed random networks with entries 0, 1 and  $-1$  have also been studied analytically and numerically in Ref. [26]. In Ref. [26] eigenvalues spectra of large random matrices with excitatory and inhibitory columns drawn from a distribution with different means and equal or different variances have been computed. Interestingly, the spectra of these random matrices (with 0 and 1,  $-1$  entries) also follow Girko's circle law.

The main goal of the present work is to investigate the changes in the spectral properties of the corresponding matrix as the underlying directed network deviates from the perfect community structure. Furthermore, in order to understand the origin of delocalized eigenvectors, we track the spectra as directionality is introduced into the networks, i.e. connections are made directed with probability  $\tau$ . Apart from the spectral distribution we study eigenvectors localization properties of model networks and a realworld networks.

## II. MODEL

We generate networks with a community structure as follows. First,  $m$  Erdős-Rényi random networks [27] with connection probability  $p$  are constructed; the spectral behavior of the matrix corresponding to each of these sub-networks (blocks) separately follows GOE statistics [12]. The matrix corresponding to the full network would be

an  $m$  block diagonal matrix. Then, with probability  $p_r$  connections are rewired as follows. A pair of nodes from a sub-network is chosen randomly. Subnetwork is also chosen with equal probability. The connection between these two nodes is deleted, and a new connection between one of the node in the chosen pair and a randomly chosen node outside to this sub-network is introduced. This configuration leads to an  $m$  block matrix with, blocks having entries 1 with probability  $p$ , and off-diagonal blocks having the entries 1 with probability  $p_r$ . The above networks can be casted in the following form:

$$A = A_0 + A_{p_r} \quad (1)$$

where  $A_0$  is the direct sum of all the blocks ( $A_0 = A_1 \oplus A_2 \oplus \dots \oplus A_m$ ). The directionality of the edges is introduced as follows. A node is assigned equal probability of being inhibitory or excitatory. All edges starting from an excitatory node would take value 1, and those starting from an inhibitory node would take the value  $-1$ . This means that the corresponding adjacency matrix  $A$  has entries as follows: if the  $i$ th node is excitatory,  $A_{ij} = 1$  for all the  $j$  nodes that have connections with  $i$ , and if the  $i$ th node is inhibitory,  $A_{ij} = -1$ . The corresponding matrix has following two properties: (a)  $|A_{ij}| = |A_{ji}|$ , and (b) a row has all entries either 1 or  $-1$ . This configuration would lead to zero mean ( $\sum_{i,j} A_{i,j} \sim 0$ ), and standard deviation  $\sigma^2 \sim \tau$ . We denote the eigenvalues of network by  $\lambda_n$ ,  $n = 1, \dots, mN$ , where  $N$  is the size of sub-network, and  $m$  is the number of sub-networks. Note that the size of each sub-network may be different, but for simplicity we consider equal size here.

Connections are rewired with the probability  $0 < p_r < 1$ , where  $p_r$  defines the ratio of inter-community ( $N_{inter}$ ) to intra-community ( $N_{intra}$ ) connections. Starting with two ER sub-networks of dimension  $N$ , a fraction  $p_r$  of the connections is rewired. The average degree of network for each  $p_r$  remains the same as that of the initial configuration. Nodes are inhibitory or excitatory with equal probability, which implies an approximately equal number of 1 and  $-1$  entries randomly distributed in the corresponding matrix. For  $p_r \sim 0.5$ , the whole structure becomes a directed random network, and for  $p_r \sim 1$  which indicates that all the connections are rewired, the network takes the form where nodes in  $A_1(A_2)$  are connected to those in  $A_2(A_1)$ .

### III. SPECTRA

In the following we present the results for  $N = 1000$ ,  $m = 2$ , and  $p = 0.02$ . The average degree of the network can be calculated as  $\langle k \rangle \sim pN = 20$ . The eigenvalues spectra of  $A_1$  and  $A_2$  for  $p_r = 0$  follow Girko's law of non-Hermitian matrices [17]. We numerically diagonalize the adjacency matrix of the network to obtain a set of eigenvalues  $\lambda_k = R_k + iI_k$ , and eigenvector  $\psi_i$ . To characterize the localization properties of the eigenvectors  $\psi_i$ ,

we use the inverse participation ratio (IPR) defined by,

$$I_i = \frac{(\sum_j |\psi_i(j)|^2)^2}{\sum_j |\psi_i(j)|^4} \quad (2)$$

where  $\psi_i(j)$ ,  $j = 1, \dots, N$  are the components of the eigenvector  $\psi^i$ . The meaning of  $I$  is illustrated by two limiting cases : (i)  $I_i = N$  for a vector with identical components  $\psi_i(j) \equiv 1/\sqrt{N}$  whereas (ii)  $I_i = 1$  for a vector with one component  $\psi_i(j) = 1$  and the remainders zero. Thus, the IPR gives the effective number of nodes on which an eigenstate is localized.

Figure (1) plots eigenvalues together with the IPR for the model described in the section II. Subfigures correspond to different rewiring probabilities. For each rewiring probability eigenvalues are distributed homogeneously in a circular region. Gray shading (color) denotes the value of IPR for the corresponding eigenstate. For Figure (1 a) with  $p_r \sim 0$ , which corresponds to the network having two communities connected with one single connection, large number of eigenstates have approximately equal IPR value close to the bottom of the shading (coloring). Few eigenstate lying at the boundary of the circle and a few near the real axis have low IPR values, indicating high participation in the localization.

Figure (1) plots the results upto rewiring probability  $p = 0.01$ , as rewiring is increased further the spectral distribution remains exactly the same as for  $p = 0.01$  case except that the light gray (green) hazy circular part becomes bigger and denser indicating that more eigenvalues are delocalized. As rewiring keeps on increasing, leading to the destruction of the community structure more and more eigenvalues join the light gray (green) big circle, and for  $p_r = 0.1$  except for a few eigenvalues lying at the end of the real and imaginary axes all are delocalized. Additionally, the eigenstate near the real axis has relatively lower IPR values. One eigenvalue lying at the extreme end of the real axis is the most localized. For a further increase in rewiring probability there is not much of a change in the localization properties of eigenstates. The value  $p_r = 0.5$  corresponds to the same expected number of intra and inter-community connections. At this value the network is a complete random network. A further increase in  $p_r$  takes the network toward a bipartite type of structure.

#### A. Fine rewiring

Figure (1) shows that the localization properties of a network change completely even for a very small value of  $p_r$ , as small as  $p_r = 0.1$ . After this value no visible changes are seen in the localization properties of the bulk of the spectra. To gain insight into the localization to delocalization transition we track the spectra for each rewiring between the communities (Eq. 1). First four subfigures (Figure 1 a - 1 d) plot the spectra along with the localization value for a very small number of

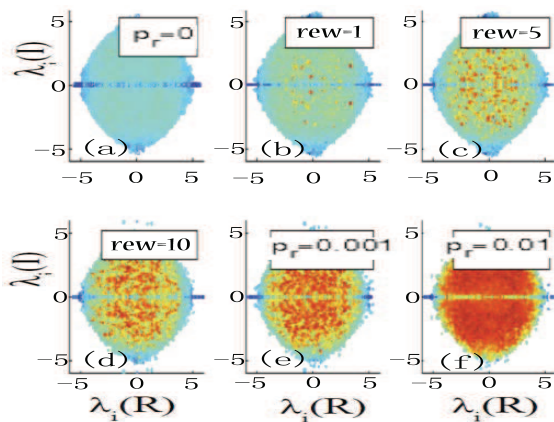


FIG. 1: (Color online) Spectra with IPR for networks starting with two communities of size  $N = 1000$  and then rewiring connections between communities with different probabilities. Average degree is  $\langle k \rangle = 20$ . The real and imaginary parts of the eigenvalues are plotted on the x and y axes, respectively. (b) One and (c) five rewirings are plotted for an ensemble average of 100. For other rewiring probabilities the spectra are plotted for an ensemble average of 10. The rewiring probability is denoted by  $p_r$ . The value of the IPR varies from (a)-(f)  $I = 0$  [dark gray, blue, patches at the corners] to (b)-(f)  $I = 1100$  [dark gray, red, points inside the circular region]. Light gray regions inside the circle in (a) - (c) depict less delocalization than the dark gray patches at the corners. Light gray area inside the circular regions and the horizontal line at x axis of (d)- (e) are even less delocalized than the peripheral light gray areas that have the same level of delocalization as the interior of (a)-(c).

rewiring All figures are plotted for an ensemble over 100 random initial conditions for the networks. Figure (1 a) plots the spectra and IPR value for a perfect community network without any connections between them. This configuration leads to two

disconnected components. With only one rewiring between two communities, we already start observing the delocalization of few eigenstates (Figure 1 b). Each additional rewiring between communities leads to the delocalization of more eigenstates. For as few as 10 rewiring to the initial configuration (Figure 1 a) a large number of eigenstates are delocalized (Figure 1 d). One can notice in Figure (1) that delocalized eigenstates form a hazy ring around center [26]. Eigenstates lying at the peripheral of the circle and those corresponding to the real axis delocalized in last for very large value of rewiring probability between the communities. For  $p_r = 0.01$ , eigenstates near real axis and with large absolute values are those which still maintain localization. As value of  $p_r$  increases further except few eigenstates having largest absolute values lying at real and imaginary axis are delocalized. Bulk middle part delocalized completely. As value of  $p_r$  increases further, bulk middle part remains same, only eigenstates with largest absolute eigenvalues at imaginary axis are more delocalized. For  $p_r \sim 0.9$ , the spectra remains similar to that of value  $p_r = 0.1$ .

We would like to note that spectral properties of  $m$  coupled *GOE* random symmetric matrices have been investigated in details. They have been used to understand the behavior of quantum graphs [28].

#### IV. COMPARISON WITH RANDOM NETWORKS

In order to gain insight into community induced spectral changes, we present results of random networks. In the following we first provide the eigenstate properties of random networks having different average degrees, and then track the spectral properties as parameters of  $\tau$ .

##### A. Completely uncorrelated (directed) network

First we consider completely uncorrelated random networks, for which  $\tau = 0$  and the connection probability is  $p$ . Since there is equal probability of a node being inhibitory or excitatory, the expected number of 1 and  $-1$  entries is approximately same. The mean and variance of this network can be calculated as  $\mu = 0$  and  $\sigma^2 = p$ , respectively.

Figure (2) plots eigenvalues together with the IPR for random networks with different connections probabilities.

As we do not consider self connection, the diagonal elements of the matrix are zero, and hence eigenvalues are distributed around origin 0. Eigenvalues are distributed in circular region of radius  $\sqrt{Np(1-p)}$ . For larger values of  $p$ , few pairs of eigenvalues get separated from the circular bulk. The bulk circular region still lie between  $-\sqrt{Np(1-p)}$ ,  $\sqrt{Np(1-p)}$ . For  $p = 1$  which corresponds to globally coupled network, there is one conjugate pair of eigenvalues with absolute value  $\sqrt{N}$  which are nondegenerate, rest of eigenvalues are degenerate with values 1 and  $-1$ .

Different connections probabilities lead to different expected average degree of the network. For low connection probability,  $p = 0.005$ , one gets localized eigenstates at four corners of the real and imaginary axis. Apart this four corners the eigenstates on real axis are also more localized. As connection probability increases overall distribution of eigenvalues remains same, i.e. homogeneous, except for larger  $p$  few pairs of eigenvalues get separated from the bulk circular region [19]. Except eigenstates lying on real axis, other eigenstates are toward dark gray (blue) denoting delocalization. The isolated eigenstates are maximal delocalized, which implies that eigenstates having large absolute eigenvalues are more random than the bulk part. Very small values of  $p$  yields a delocalized spectra (Figure 2 a), which may be due to the sparseness of connections.

Here we would like to mention that, the above behavior is for the special arrangement of 1 and  $-1$  entries in the matrix, a row has all 1 or  $-1$  entries depending

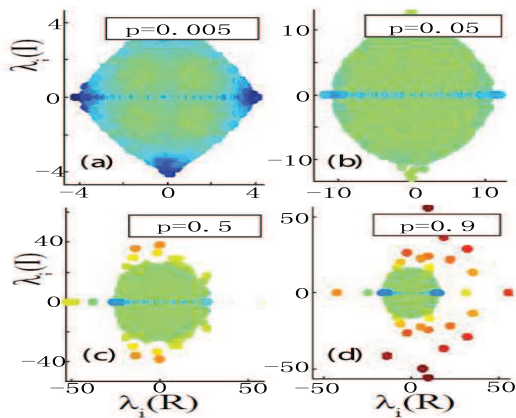


FIG. 2: (Color online) Spectra with the IPR for directed random networks having different connection probabilities  $p$ . The size of the networks  $N = 2000$ , and spectra are plotted for 10 random realizations for each value of  $p$ . The real and imaginary parts of the eigenvalues are plotted on the x and y axes, and gray shading (color) denotes the value of the corresponding IPR. The value of the IPR varies from  $I = 0$  [dark gray, blue, patches in corners of (a)] to  $I = 2000$  [scattered dark gray, red, dots in (d)]. Light gray areas inside the circular regions in (a)-(d) are less delocalized than the dark gray patches in (a). Light gray dots outside the circular region in (c) are not as delocalized as the light gray regions described earlier. Darker gray dots outside the circular region in (c) and (d) are not as delocalized as the light gray dots in the same region and are more delocalized than the dark gray dots in (d), which are more the localized. Note the scale of the gray shading (color) axis for this case, which is different from other figures. (a)-(d) The horizontal line at x-axis shows the same level of localization as the value of delocalization close to the most delocalized eigenstates.

upon whether the corresponding node is excitatory or inhibitory. For a random network with entries 1 and  $-1$  randomly distributed, the radius of circular region scales with average degree of the network, i.e.  $\sqrt{pN}$ , and all eigenvalues lie within the bulk regions even for larger value of  $p$  including  $p = 1$ .

For random symmetric networks ( $\tau = 1$ , in Eq.4) with mean  $p$  and variance  $p(1-p)$ , the distribution of the largest eigenvalue is given by the results in [29], which shows that for constant  $p$  the distribution of the principal eigenvalue of the random network is asymptotically normal with mean  $Np + (1-p)$  and variance  $2p(1-p)$  as  $N \rightarrow \infty$ . For asymmetric random networks the corresponding result for the distribution of largest eigenvalue has yet to be found, but in [30] it was shown that asymmetric network of 0 and 1 entries and having mean  $p$  and variance  $p(1-p)$ , the principle eigenvalue asymptotically converges to  $Np$ . For matrices with entries 1 and  $-1$ , the mean and variance differ from above, as mean and variance for completely uncorrelated random network ( $\tau = 0$ ) with parameters  $N, p$  would be 0 and  $p$  respectively.

Though the IPR is, in general, used to understand the localization property of individual eigenstates, the sum

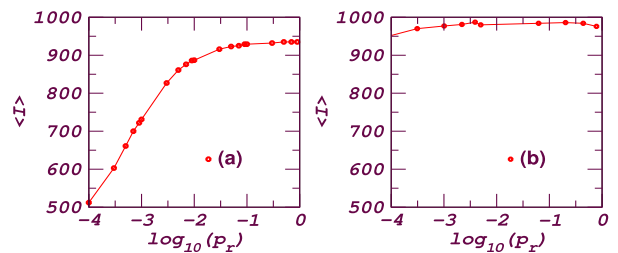


FIG. 3: (Color online) The IPR for (a) random network with the community as in Figure 1 as a function of the connection probability between communities  $p_r$ ,  $N = 2000$  and average degree  $\langle k \rangle = 20$  (b) a random network,  $N = 2000$  as in Figure (2), as a function of  $p$  or average degree  $\langle k \rangle$ .

of all  $I_i$

$$\langle I \rangle = \left\langle \sum_i I_i \right\rangle, \quad (3)$$

where bracket means ensemble average, can be used as a measure for localization properties of whole spectra altogether [28]. We calculate the total value of IPR  $\langle I \rangle$  in order to get a measure of localization for the whole network. Figure (3) plots  $\langle I \rangle$  for a random network with a community structure for an increasing value of the connection probability between communities. In a straight forward manner, the figure shows delocalization in the whole spectrum with deformation from the community structure. The value of  $\langle I \rangle$  increases, which means that overall the spectrum becomes more delocalized until a certain value of rewiring probability  $p_r \sim 0.005$  and then becomes saturated, as shown in Figure (1). The localization properties of spectra are barely distinguishable from the community structure for larger value of deformation. The figure is plotted for network size  $N = 2000$  and average degree  $\langle k \rangle = 20$ . We also plot the IPR (3) of random networks for various value of  $p$  or an average degree  $\langle k \rangle$ . The network size always remains the same,  $N = 2000$ . The range for  $p$  is from  $p = 0.001$  to 0.9. We do not plot the graph below  $p \sim 0.001$ , since for  $N = 2000$ , smaller values of  $p$  yield several disconnected clusters.  $N = 2000$  and  $p \sim 0.001$  yield an average degree  $\langle k \rangle \sim 20$ .

### B. Tracking from correlated (symmetric) to a completely uncorrelated (asymmetric or directed) network

In this section we investigate the origin of localization or delocalization of eigenstates by tracking the spectra as connections are made undirected. We start with a network having all nodes excitatory leading to a symmetric network, now with probability  $(1-\tau)/2$  some nodes are made inhibitory.  $\tau = 0$  corresponds to the case when half of nodes are made inhibitory, leading to a completely

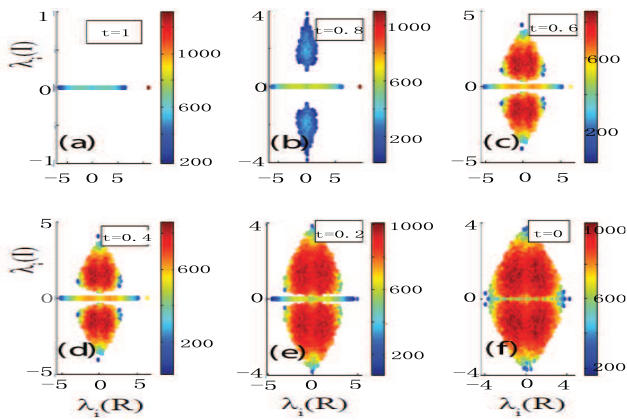


FIG. 4: (Color online) Spectra with the IPR for random networks having different values of  $\tau$ . (a)-(f) The size and average degree of the network are  $N = 2000$  and  $\langle k \rangle = 10$  respectively. For a symmetric network,  $\tau = 1$ , and  $\tau = 0$  corresponds to complete asymmetric network (see the text). The value of the IPR varies from  $I = 0$  [dark gray, blue, at the bottom of shading scale] to  $I = 1300$  [dark gray, red, at the top of the scale]. Dark gray points at both ends of the line at  $x = 0$  and dots at the periphery of the two circular region on both sides of the real axis correspond to  $I = 0$ , whereas a dark gray dot separated by other eigenvalues in (a) and (b), and dark gray patches inside the circular region in (c)-(f) correspond to  $I = 1300$ . Gray shading in (b) denotes different levels of delocalization from  $I = 0$  (dark gray) to  $I = 600$  (light gray), whereas in (c) and (d), gray shading in the circular region denotes the localization value from  $I = 1000$  (dark gray) to  $I = 600$  (light gray), with other gray shading for the intermediate values. Light gray regions in the middle of the real axis and toward the top and bottom of the circular regions in (c)-(f) correspond to the middle of the scale, whereas the darker gray region in (c) and (d) correspond to the value  $I = 800$  in the gray scale.

uncorrelated network. As  $\tau$  fraction of connections are made symmetric, the mean and variance take form as:

$$\begin{aligned} \mu &= \sum_{ij} A_{ij} \sim \tau p \\ \sigma^2 &= \sum_{ij} (A_{ij} - \mu)^2 \sim p(1 + \tau p - 2\tau^2 p) \end{aligned} \quad (4)$$

$\tau = 1$  corresponds to a symmetric network which we call as a complete deviation from the directed network, i.e.  $A_{i,j} = A_{j,i} \forall i \& j$ . We call "deviation from directionality" because as one deviates from completely directed networks, spectra deviate from the circular structure. For a network, where nodes are inhibitory or excitatory with equal probability,  $\langle A_{ij} \rangle = 0$  and  $\langle A_{ij}^2 \rangle \sim p$ .

Figure (4) plots the spectra along with the IPR values for random networks for different values of  $\tau$ . The largest eigenvalue lies on real axis well separated from the bulk. Isolation of largest eigenvalue from rest is well known observation for real symmetric random matrices having non zero mean [31]. It was proved in [31] that such an isolated eigenvalue exists for a large matrix if the mean value of

the elements is not zero and rather carries substantial fraction of the root mean square of the elements. Furthermore, the associated eigenvector would have all its components close to equality.

Now let us first consider the case with  $\tau = 1$ . The corresponding matrix would be a symmetric matrix with  $pN(N-1)$  entries being 1 and rest being 0, the mean and variance of this matrix can be calculated as  $\mu = p$  and  $\sigma^2 = p(1-p)$  respectively (Eq. 4). The largest eigenvalue of the matrix scales as  $pN$ , which is equal to the average degree of the network. Rest of the eigenvalues are homogeneously distributed in a circular region of radius  $pN(1-p)$ . As connections are made directed, the mean  $\mu$  decreases, and for  $\tau = 0$ , mean takes value 0, and variance is simply given by  $p$  which is connection probability. As connections are made directed, eigenvalues start appearing in complex conjugate pairs, and we can divide spectra into two parts: (A) part of spectra with real eigenvalues, and (B) the part of spectra having complex conjugate pairs of eigenvalues. For  $\tau = 0.8$ , which means 20% of connections are made directed, many eigenvalues are still in group (A), i.e., they lie on real axis. Complex conjugate pairs of eigenvalues form an oval shape that is well separated from real axis (see Figure (4)). The localization properties of eigenstates from both the groups do not change much, as bulk part which is separated from the real axis is still delocalized, only middle part of eigenstates lying at the real axis (group (A)) delocalized than a completely symmetric network. As more connections are made directed, complex conjugate pairs of eigenvalues start appearing with delocalized states. Bulk of the complex conjugates pairs lying at both sides of the real axis and forming oval shape (group (B)) are delocalized, only few eigenvalues in this group with largest absolute value remain localized. Eigenvalues forming group (A) also show similar features as group (B), eigenstates with larger eigenvalues at both ends remain localized, whereas rest of the eigenstates are more delocalized than earlier.

As more connections are made directed (value of  $\tau$  is decreased), size of group (B) keeps increasing, and consequently two parts of eigenstates come closer. For  $\tau = 0.2$ , group (B) is no longer separated from the eigenstates lying on the real axis (group (A)).

Figure (5) plots the total  $\langle I \rangle$  (Eq.3) for a particular value of connection probability  $p = 0.01$  and network size  $N = 2000$ . Starting from a symmetric network ( $\tau = 1$ ), connections are made directed with probability  $(1 - \tau)$ . Overall spectral delocalization increases as connections are made directed leading to occurrence of complex conjugate pairs of eigenvalues in spectra. Delocalization reaches its maximum for  $\tau = 0$  value which corresponds to a complete uncorrelated or directed network. For networks having only positive entries, there is not much change in the localization properties till value  $\tau \leq 0.8$ , after this there is a sharp decay in  $\langle I \rangle$  indicating sudden localization transition. For values between 0 and 0.8, spectral distribution smoothly changes from circular to elliptical, localization property does not show

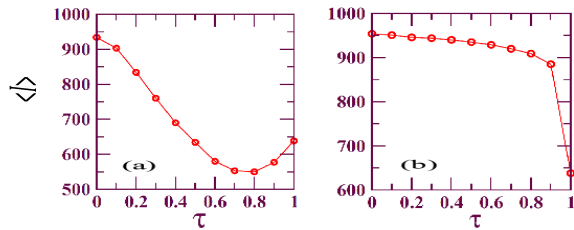


FIG. 5: (Color online) The total IPR as a function of  $\tau$ . The data are plotted for  $N = 2000$ ,  $\langle k \rangle = 20$  and for 10 ensemble averages of the random networks. (a) Networks with inhibitory and excitatory nodes leading to 1 and  $-1$  entries in the corresponding matrix, and (b) random network with only excitatory nodes leading to only 1 entries in the corresponding matrix.

any rich structure, as shown for the previous case.

### C. Random networks with positive entries

In the above we investigated networks with both excitatory and inhibitory connections. This section considers all nodes being excitatory, and consequently the adjacency matrix has all positive entries only. For asymmetric random network of 0 and 1 entries, with mean  $p$  and variance  $p(1-p)$ , the principle eigenvalue asymptotically converges to  $Np$  [30]. The rest of the eigenvalues are distributed in circular region with radius given by  $\sqrt{Np(1-p)}$ . In this section we present the spectral changes as network goes from an asymmetric (directed) corresponding to  $\tau = 0$ , to a symmetric network corresponding to  $\tau = 1$ . The mean and variance for networks with entries 1 would not depend on the value of  $\tau$ , and depends only on connection probability  $p$  as

$$\begin{aligned} \mu &= p \\ \sigma^2 &= (1-p) \end{aligned} \quad (5)$$

Figure (6) shows spectra along with localization property for different values of  $\tau$ . Spectral distribution smoothly goes from circular distribution to elliptical as value of  $\tau$  increases. For all values of  $\tau$ , the largest eigenvalue is completely delocalized, and situated very well separated from the rest bulk part with value  $\lambda_{max} \sim Np$ , as for the case  $\tau = 0$ . Note that for each value of  $\tau$ , the expected number of entries 1 remains same for a fixed  $p$  value.

## V. NETWORKS WITH SCALEFREE COMMUNITY STRUCTURE

In this section we consider that each community is modeled by a scalefree network instead of a random net-

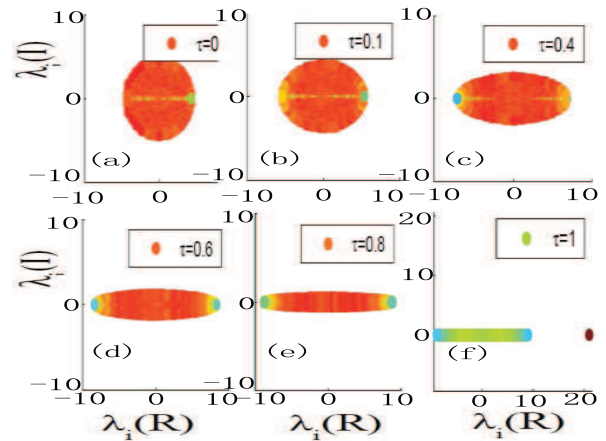


FIG. 6: (Color online) Random network for various values of  $\tau$  but with only excitatory coupling. The network size  $N = 2000$  and the average degree  $\langle k \rangle = 20$ . The value of the IPR varies from  $I = 0$  [light gray, blue, at the two ends of the spectra on the x axis] to  $I = 1200$  [dark gray, red, circular regions]. the light gray region in the middle of x-axis in (f) is not as delocalized as the light gray points toward both ends. The light gray horizontal line at x axis in (a)-(c), and the light gray patches at the corner of (b)-(e) have the same level of localization, which shows less delocalization than the light gray region in (f) described above.

work. Each sub-network has size  $N = 1000$  and average degree  $\langle k \rangle = 20$ , and is constructed using BA preferential attachment rule [10]. With probability  $p_r$  intra-community connections are rewired into inter-community connections. Connections are made directed in same manner as given in the section II.

Spectra of the above construction are plotted in Figure (7). The first difference between the spectra of these networks from those having a random community structure (II) is that the eigenvalues are not homogeneously distributed in the circular region. The spectra are more dense around origin, and sparser near boundary. Also the value of largest absolute eigenvalue increases, as the highest degree of the node in the current structure are very much larger than that of the previous structure (II). Localization property overall remains same as those of the networks discussed in II.

## VI. COMMUNITY STRUCTURE : TRACKING FROM SYMMETRIC TO A COMPLETE ASYMMETRIC (DIRECTED) NETWORK

In this section we investigate the origin of localization or delocalization properties of eigenstates for networks having distinguished community structure. Particularly we concentrate on the community dependent localization features as connections are made directed, and compare them with random networks features presented in the section IV B. Starting with  $m = 2$  random symmetric sub-networks with  $p_r = 0.2$  rewiring probability between

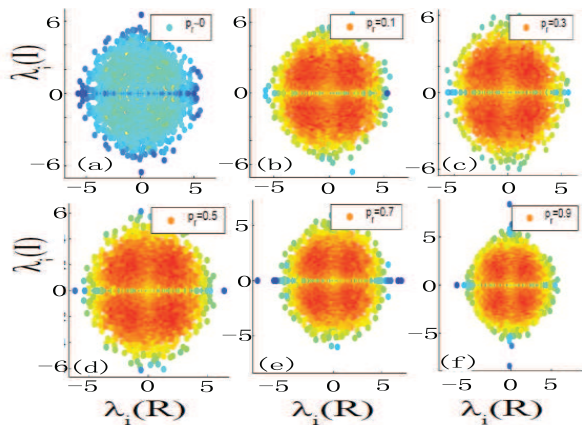


FIG. 7: (Color online) Eigenvalues with the IPR for networks having two scalefree sub-networks, and for different rewiring probabilities. The size of each community  $N = 1000$  and the number of communities is  $m = 2$ . The average degree is  $\langle k \rangle = 20$ . The rewiring probability is denoted by  $p_r$ . The value of IPR varies from  $I = 0$  [dark gray, blue, scattered points at the peripheral of all sub-figures and a few points separate from the bulk in (d)-(f)] to  $I = 1200$  [dark gray, red, patches in the middle of (b)-(f)]. Gray shading in (a) shows different levels of delocalization with dark gray being the most delocalized to lighter gray being less delocalized. Light gray points at the periphery in (b)-(f) are not as delocalized as the light gray region inside the circle of (a), whereas they are more delocalized than the light gray region inside the circle in (b)-(f).

these sub-networks, connections are made directed with the probability  $\tau$  as explained in the previous section. Again,  $\tau = 0$  corresponds to a fully directed network such as explained in II, and  $\tau = 1$  corresponds to the symmetric network. A symmetric random network with connection probability  $p$  has mean  $p$  and variance  $p(1-p)$ , whereas mean and variance of a fully directed network (made of 1 and  $-1$ ) are 0 and  $p$  respectively. Probability of directed connections ( $\tau$ ) affects the mean and variance as given in Eq. 4.

Figure (8) plots the eigenvalue spectra combined with the IPR as  $\tau$  varies from  $\tau = 1$  (a perfect symmetric case) to  $\tau = 0$  (a uncorrelated case). Subfigure (a) corresponds to the configuration when almost 80% nodes are excitatory leading to very large correlation among entries of the matrix. For very small number of directed connections the spectra have mostly real eigenvalues, and eigenstates are localized. As number of directed connections increases spectra have more complex eigenvalues. Subfigure (i) corresponds to the case where  $\sim 80\%$  of nodes are inhibitory, which is exactly the same case in terms of correlations as shown for subfigure (a) except that the corresponding network has dominating  $-1$  entries.

As similar to the section IV B, spectra can be divided into two parts, (A) part of spectra lying on the real axis, and (B) the part which form complex conjugate pairs. The appearance of complex eigenvalue seems to be an indicator of delocalization transition. For small number

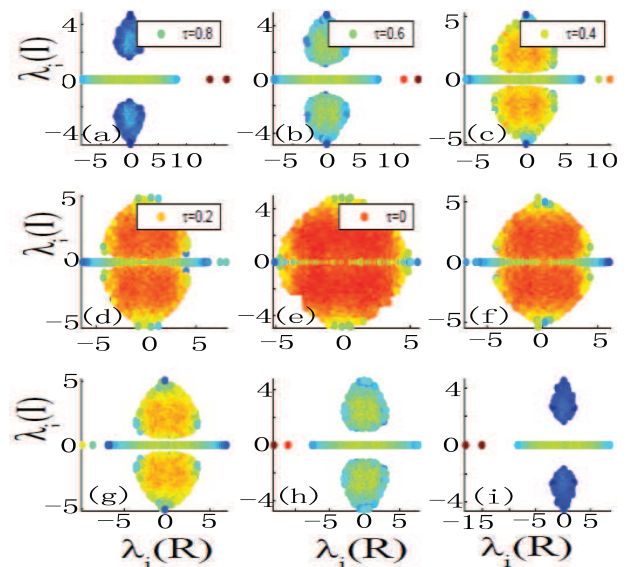


FIG. 8: (Color online) Spectra with the IPR for networks having two random sub-networks, and for  $p_r = 0.2$  rewiring probability. The size of each community  $N = 1000$  and the average degree  $\langle k \rangle = 20$ . The different probabilities of directed connections are plotted (see the text). Configurations are shown in which (a)-(d) excitatory nodes are dominant, (f)-(i) inhibitory nodes are dominant, and (e) there is equal probability of a node being excitatory or inhibitory. The value of the IPR varies from  $I = 0$  [dark gray, blue, patches at the periphery of both circular regions on two sides of the real axis in (a) and (i), and dark gray points toward both ends of the real  $x$  axis in (c)-(g)] to  $I = 1200$  [dark gray, red, points well separated from bulk in (a)-(i)]. Gray shading in (a),(b), (h) and (i) denotes different levels of delocalization with dark gray (except two dots well separated from the bulk) denoting maximum and light gray showing minimum delocalization. Light gray area inside the circular regions in (c) and (g) show less delocalization than the light gray area in (a) and (b). Dark gray area inside the circular regions in (c) - (g) show less delocalization than the similar dark gray area inside the circular region of (a).

of directed connections (Figure 8 a) most of the eigenvalues are real and hence localized. As more connections are made directed, complex pairs of eigenvalues start appearing and eigenstates associated with these complex values start getting delocalized. For  $\tau = 0$ , which leads to a complete asymmetric or directed network, one gets complex pairs of eigenvalues covering the whole circle, and hence almost all eigenstates, except those associated with real eigenvalues and those with maximum absolute value, get delocalized.

Now, as we compare the spectra of above construction with those of random networks, we observe one remarkable difference revealing two communities hidden in the network. For small number of directed connections (i.e. large values of correlation parameter  $\tau$ ), there are exactly *two* isolated eigenvalues on the real axis well separated from the bulk. Figure (8 a) shows that these isolated eigenstates corresponds to two largest eigenvalues



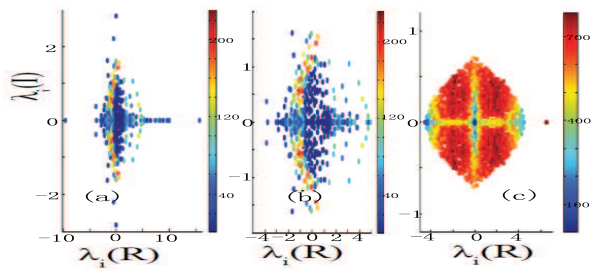


FIG. 9: (Color online) (a) Spectra of the zebrafish metabolic network. (b) Close-up of the spectra. (c) Spectra of the random network with same parameters (i.e. number of nodes, and number of directed and undirected edges) as zebrafish metabolic network. Gray shading (color) denotes the localization properties of the corresponding eigenvalues. Dark gray (blue) patches in (a)-(b) and dark gray dots at the end of the real axis as well as at the center of (c) correspond to the bottom of the gray shading with an IPR value  $I = 0$ , whereas dark gray (red) patches inside the circular region in (c) and a dark gray dot well separated from bulk lying at extreme right correspond to the top of the shading scale with an IPR value  $I = 800$ . The light gray vertical regions toward the left side in (a) and (b) is not as delocalized (with an IPR value close to 500, as in the scale) as the light gray vertical region toward the right side of the same plot (with an IPR value varying by about 300 in the scale). Similarly, light gray points at the right corner of (c) are more delocalized than the part of the vertical and horizontal gray area of similar shade crossing at center. Darker gray patches in (c) are not as delocalized as the patches with the same shade in (a) and (b).

and both of them are delocalized. For  $\tau = 0.6$ , which means that number of directed connections is higher than  $\tau = 0.8$ , these isolated eigenvalues still exist on the real axis but come closer to the rest bulk part. Further increase in the number of directed connections brings isolated eigenvalues even closer, as well their localization properties get affected. For  $\tau = 0.4$ , these isolated eigenvalues are no more extended, and eigenstates having largest absolute values from group (A) and (B) are most localized. As  $\tau$  is decreased further, these isolated eigenvalues merges with the bulk part of group (A).

## VII. ZEBRAFISH METABOLIC NETWORK

This section compares the behavior shown by the model networks discussed so far with a realworld network. We use network for the zebrafish metabolic system. The network is constructed by using the KEGG data base [32]. Nodes in the network are reactions. If the product of one reaction (say A) is the substrate of another reaction (say B) then there is a directed link from A to B. There are also some directed links that correspond to the irreversible biochemical reactions. The largest connected component of the network has  $N = 1593$  nodes and  $E = 9018$  edges. The number of undirected edges is 6770 and the number of directed edges is 2248. The

value of  $\tau$  can be calculated as  $\tau = 6670/9018 \sim 0.7$ . The average degree of the network is  $E/N \sim 6$ . Figure (9) plots the spectra of this network. In order to compare the results with a corresponding random network, we plot Figure (9 c) spectra of a random networks ensemble with the same size and number of directed and undirected edges as in the zebrafish network.

We notice that the spectrum of the zebrafish network has few drastic differences from those of model networks discussed in the preceding sections. The main observation is the clustering of eigenvalues in an elliptical disk along the imaginary axis. Two extremal eigenvalues lie on the real axis, and they are far from the rest of the bulk eigenvalues. The corresponding random network also has the largest eigenvalue situated at the real axis with a value close to the average degree of the network. This eigenvalue is situated far from the rest of the bulk eigenvalues centered around zero. This is a typical spectral behavior of directed random networks, as discussed in the Sec. IV.

Furthermore, the localization properties of eigenstates of the real networks studied show very different phenomena than what observed for the corresponding model networks. In an elliptical disk there is one layer of eigenstates that are very much localized, and the second layer in the disk shows a full range of IPR values between extreme localization and extreme delocalization. There are many eigenvalues that lie on the real axis, which can be explained by the relation between asymmetry in the matrix and the occurrence of complex eigenvalues discussed in Sec. VI (Fig. 8). However the localization properties of these eigenstates corresponding to the real axis are different than the corresponding model network and other earlier model networks we investigated in the preceding sections. The main difference is that all eigenstates lie toward the bottom on the localization scale. The isolated eigenvalues for model networks so far are observed with the most extended state, whereas for the zebrafish network, the isolated eigenvalue lies toward bottom of the localization value.

## VIII. CONCLUSION AND DISCUSSIONS

We analyzed the spectral properties of various model directed networks and a realworld network. The network edges take value 1 and  $-1$  depending upon whether it is starting from an excitatory node or from an inhibitory node. If all nodes are excitatory then the corresponding network is symmetric ( $\tau = 1$ ). Directionality is introduced by making some nodes inhibitory, and consequently the corresponding edges take value  $-1$ . An equal expected value of inhibitory and excitatory nodes gives rise to a completely uncorrelated network ( $\tau = 0$ ).

Asymmetric networks ( $\tau = 0$ ) with a community structure modeled by a random sub-network show circular spectra similar to random uncorrelated matrices. Spectra for networks with entries 1,  $-1$  follow Girko's circular

distribution with radius  $\sqrt{pN(1-p)}$ . For a very well distinguished community structure  $p_r \sim 0$ , the whole spectrum is localized except for some of eigenstates at the boundary. As  $p_r$  increases and the network deviates from a community structure there is a sudden change in the localization property for a very small value of deformation from the perfect community structure. The value as less as  $p_r \sim 0.1$ , which corresponds to only 10% inter-community connections (Fig. 1), gives rise to a delocalized spectrum. In order to understand this delocalization transition we track the spectra for very fine rewiring between communities (Fig. 1). For exactly one rewiring most of the eigenvalues lying on the real axis are delocalized. This suggests that there are eigenfunctions confined within their respective random communities. With the increase in rewiring between communities some of the eigenstates lying at the boundary of the circular region start delocalizing. This suggests that some of the eigenstates now span the whole network through rewired connections that connect two sub-networks. With the further deformation from the community structure, the next level of delocalization starts occurring through a circular ring around center, which gradually spans the whole spectrum with an increase in the rewiring.

The spectra of random networks, where the probability for a node being inhibitory or excitatory is equal, show a circular distribution with a radius  $\sqrt{pN(1-p)}$ . Based on the IPR values, the spectrum can be divided into two parts, (A) one part consisting of eigenstates at the real axis and at four corners with large absolute eigenvalues that are localized, and (B) another part consisting of the bulk middle part of the spectrum, which is less localized. As the connection probability increases part (B) starts dominating the spectra, except for a few localized eigenvalues, which remain very well separated from the bulk part even for very large connection probabilities.

In order to understand the mechanism for localization we tracked the spectra as the network is rewired from a completely symmetric structure ( $\tau = 1$ ) to a completely asymmetric one ( $\tau = 0$ ). For symmetric networks spectra lie on the real axis with exactly one eigenvalue separated from the bulk. As connections are made directed by making some nodes inhibitory, some of the eigenstates start occurring in complex conjugate pairs. The eigenvalue distribution along with the IPR value show a rich pattern. Overall, the spectra gradually become more delocalized as the number of directed connections increases.

Furthermore we studied spectra of matrices with non-negative entries. This kind of matrices was previously investigated in details; we also showed that the spectral distribution follows Girko's generalized law. For  $\tau = 0$  it shows circular distribution, and as the correlation  $\langle A_{ij}A_{ji} \rangle$  increases spectra become elliptical. The localization properties of whole spectra remain similar except for a sudden localization for very large values of  $\tau$ .

Spectra of networks with a scalefree community structure do not show a localization pattern that is much dif-

ferent from spectra of networks with the random community structures. For two separated communities with one connection between them, the spectra are circular with radius  $\sqrt{pN(1-p)}$  and the boundary of the circular region is scattered. As more connections are rewired leading to stronger coupling between the communities, the spectral distribution remains same but the localization behavior of the eigenstates changes. The main difference from the spectra of networks in section Sec. II is that they are less delocalized which is obvious because any network with a scalefree community structure always has more structure than the corresponding networks with a random community structure. The crucial point is that the spectral distribution is very robust with the changes in the structure of the network and depends strongly on the directionality measure  $\tau$ , whereas the localization property depends on both the structure of the networks and the directionality of connections, i.e., the value of  $\tau$ .

We encounter interesting features while tracking the spectra as the network with a community structure goes from a directed to a symmetric one. For a random network with two random communities, the spectrum shows exactly two eigenvalues well separated from the bulk (Fig. 1). These eigenstates correspond to the two largest absolute values and are delocalized. The largest one is completely delocalized as was the case for a random network without a community structure, but the second largest one that is well separated from the bulk provides a distinguished signature of two communities in the network. As the number of directed connections increases the spectrum can again be divided into two parts, (A) the part of the spectrum with real eigenvalues and (B) the part of the spectrum with complex conjugate pairs.

To the end we analyze a realworld spectrum. Spectral properties of the metabolic network of zebrafish show much richer features than the model networks considered in the present paper. One very striking difference is the localization property of the eigenstate with the largest absolute value. This eigenstate is localized in contrast to those of the model networks. Another observation is the clustering of eigenvalues in an elliptical disk along the imaginary axis.

In the paper we have investigated spectra and localization properties of directed networks with binary entries. The networks with inhibitory and excitatory nodes have much richer spectra than the networks with only excitatory nodes. The bulk of the spectra for completely asymmetric networks follow Girko's law, but as probability of directed connections is reduced the spectra show very different patterns depending upon the network structure and the ratio of inhibitory and excitatory nodes. The realworld network that we studied here shows a very different spectral pattern from any of the model networks we have studied. Though directed networks span a variety of complex systems, the research for directed networks leading to complex eigenvalues is limited. The results presented in the present paper provide a useful platform to understand the structural pattern in directed networks,

and can be used to investigate further the dynamical behavior of nodes relevant to a variety of problems ranging from physics to sociology.

## IX. ACKNOWLEDGMENT

We acknowledge Dr. Changsong Zhou for useful discussions at the initial phase of the work, and Zhang Xun

for providing zebrafish metabolic data from KEGG [32].

- 
- [1] M. L. Mehta, *Random Matrices*, 3rd ed. (Elsevier Academic Press, Amsterdam, 2004).
- [2] T. Guhr, A. Muller-Groeling and H. A. Weidenmuller, *Phys. Rep.* **299**, 189 (1998).
- [3] R. Grobe, F. Hakke and H.-J. Sommers, *Phys. Rev. Lett.* **61** 1899 (1988).
- [4] G. Palla and G. Vattay, *New J. Phys.* **8** 307 (2006).
- [5] J. N. Bandyopadhyay and S. Jalan, *Phys. Rev. E* **76**, 026109 (2007).
- [6] S. Jalan and J. N. Bandyopadhyay, *Phys. Rev. E* **76**, 046107 (2007).
- [7] M. A. M. de Aguiar and Y. Bar-Yam, *Phys. Rev. E* **71**, 016106 (2005); A. N. Samukhin, S. N. Dorogovtsev, and J. F. F. Mendes *ibid* **77**, 036115 (2008).
- [8] K. -I. Goh, B. Kahng, and D. Kim, *Phys. Rev. E* **64**, 051903 (2001); S. N. Dorogovtsev, A. V. Goltsev, J. F. F. Mendes and A. N. Samukhin, *ibid* **68**, 046109 (2003); E. Estrada, *Europhys. Lett.* **73** (4) 649 (2006); D. Kim and B. Kahng, *Chaos* **17** 026115 (2007); H. Yang, C. Yin, G. Zhu and B. Li, *Phys. Rev. E* **77** 045101(R) (2008); G. Zhu, H. Yang, C. Yin and B. Li, *Phys. Rev. E* **77**, 066113 (2008); G. Bianconi, arXiv:0804.1744.
- [9] S. Jalan, N. Solymosi, G. Vattay, B. Li, *Phys. Rev. E* **81**, 046118 (2010).
- [10] A.-L. Barabási and R. Albert, *Science* **286**, 509 (1999).
- [11] D. J. Watts and S. H. Strogatz, *Nature* **440**, 393 (1998).
- [12] S. Jalan, *Phys. Rev. E* **80**, 046101 (2009).
- [13] R. Albert and A.-L. Barabási, *Rev. Mod. Phys.* **74**, 47 (2002) and references therein; S. Boccaletti, V. Latora, Y. Moreno, M. Chavez, D.-U. Hwang, *Phys. Rep.* **424**, 175 (2006).
- [14] M. Girvan and M. E. J. Newman, *Proc. Natl. Acad. Sci. USA* **99**, 7821 (2002); M. E. J. Newman, *Social Networks* **27**, 39 (2005); M. E. J. Newman, *Proc. Natl. Acad. Sci. USA* **103**, 8577 (2006); M. J. Krawczyk, *Phys. Rev. E* **77** 065701 (R) (2008).
- [15] E. Ravasz *et al.*, *Science* **297**, 1551 (2002); R. Guimerá and L. A. N. Amaral, *Nature* **433**, 895 (2005).
- [16] G. Palla, I. Derenyi, I. Farkas and T. Vicsek, *Nature* **435**, 814 (2005); M. E. J. Newman, *Phys. Rev. E* **70**, 056131 (2004); A. Arenas, A. Fernandez and S. Gomez, *New J. Phys.* **10** 053039 (2008).
- [17] V. L. Girko, *Theory Probab. Appl.* **29** 694 (1984).
- [18] H. J. Sommers, A. Crisanti, H. Sompolinsky, and Y. Stein, *Phys. Rev. Lett.* **60**, 1895 (1988).
- [19] O. Giraud, B. Georgeot and D. L. Shepelyansky, *Phys. Rev. E* **80**, 026107 (2009)
- [20] B. Georgeot, O. Giraud, and D. L. Shepelyansky *Phys. Rev. E* **81**, 056109 (2010).
- [21] T. Rogers and I. P. Castillo, *Phys. Rev. E* **79** 012101 (2009).
- [22] J. J. Seidel, *Lin. Alg. Appl.* **1** 281 (1968).
- [23] J. J. Seidel, A survey of two-graphs, 481 *Proc. Internat. Coll. Teorie Combinatorie (Roma 1973)*, Accad. Naz. Lincei, Roma, (1977); J. J. Seidel and D. E. Taylor, *Two-graphs: a second survey*, 689 *Algebraic methods in graph theory, Vol. II, Conf. Szeged 1978*, Colloq. Math. Janos Bolyai 25 (1981).
- [24] Course notes by A. E. Brouwer and W. L. Haemers, available at <http://www.win.tue.nl/aeb/math/ipm.pdf>
- [25] J. G. Martin and E. R. Canfield, *SIAM J. Sci. Comput.* **31** 5, 3529 (2009).
- [26] K. Rajan and L. F. Abbott, *Phys. Rev. Lett.* **97**, 188104 (2006).
- [27] P. Erdős and A. Rényi, *Publ. Math. Inst. Hungar. Acad. Sci.* **5**, 17 (1960).
- [28] O. Hul, P. Šeba and L. Sirko, *Phys. Rev. E* **79** 066204 (2009)
- [29] B. Bollobás, *Random Graphs*, (Academic Press, London)
- [30] F. Juhász, *Discrete Math.* **41** 161 (1982).
- [31] D. W. Lang, *Physical Review* **135** Number 4B, B1082 (1964).
- [32] Kyoto Encyclopedia of Genes and Genomes (KEGG); <http://www.genome.jp/kegg/>